International Journal of Nanomedicine

Dovepress
open access to scientific and medical research

Open Access Full Text Article

ORIGINAL RESEARCH

Changes in urinary nanocrystallites in calcium oxalate stone formers before and after potassium citrate intake

This article was published in the following Dove Press journal:
International Journal of Nanomedicine
28 February 2013
Number of times this article has been viewed

Chao-Yang Duan[1]
Zhi-Yue Xia[2]
Guang-Na Zhang[2]
Bao-Song Gui[1]
Jun-Fa Xue[2]
Jian-Ming Ouyang[2]

[1]Department of Nephrology, the Second Hospital of Xi'an Jiaotong University, Xi'an, People's Republic of China; [2]Institute of Biomineralization and Lithiasis Research, Jinan University, Guangzhou, People's Republic of China

Abstract: The property changes of urinary nanocrystallites in 13 patients with calcium oxalate (CaOx) stones were studied before and after ingestion of potassium citrate (K_3cit), a therapeutic drug for stones. The analytical techniques included nanoparticle size analysis, transmission electron microscopy, X-ray diffraction, and Fourier-transform infrared spectroscopy. The studied properties included the components, morphologies, zeta potentials, particle size distributions, light intensity autocorrelation curves, and polydispersity indices (PDIs) of the nanocrystallites. The main components of the urinary nanocrystallites before K_3cit intake included uric acid, β-calcium phosphate, and calcium oxalate monohydrate. After K_3cit intake, the quantities, species, and percentages of aggregated crystals decreased, whereas the percentages of monosodium urate and calcium oxalate dehydrate increased, and some crystallites became blunt. Moreover, the urinary pH increased from 5.96 ± 0.43 to 6.46 ± 0.50, the crystallite size decreased from 524 ± 320 nm to 354 ± 173 nm, and the zeta potential decreased from –4.85 ± 2.87 mV to –8.77 ± 3.03 mV. The autocorrelation curves became smooth, the decay time decreased from 11.4 ± 3.2 ms to 4.3 ± 1.7 ms, and the PDI decreased from 0.67 ± 0.14 to 0.53 ± 0.19. These changes helped inhibit CaOx calculus formation.

Keywords: nanotechnology, zeta potential, aggregation

Introduction

Calcium oxalate (CaOx) is the major component of urinary stones. From a chemical perspective, CaOx stone formation is closely related to: high levels of urine calcium and urine oxalic acid; nucleation, growth, and aggregation of CaOx crystals; and adhesion between crystals and renal tubular epithelial cells.[1–3] Therefore, the crystallites in urine are crucial factors affecting the formation of uroliths.[4–6]

Previous studies[5,6] have found differences between the urinary crystallites (<1000 nm in size) of patients with urolithiasis and healthy subjects without any urolithiasis history. These studies concluded that the morphology, particle size, aggregation, and crystal phase of nanocrystallites in the urine of lithogenic patients remarkably differ from those of healthy persons. The urinary crystallites of healthy subjects are more stable than those of the patients. The results suggested that rounding nanocrystallites, diminishing their size differential, and decreasing their aggregation in urine by physical and chemical methods may prevent urinary stone formation.

Potassium citrate (K_3cit) is the main drug used in treating and preventing the formation of CaOx stones.[7] After K_3cit intake, the urine may be alkalized and the excretion of urinary citrate thus increases. Citrate can combine with calcium ions and form a soluble chelate that reduces the supersaturation of CaOx in urine; thus, the

Correspondence: Bao-Song Gui
Department of Nephrology, the Second Hospital of Xi'an Jiaotong University, Xi'an 710004, People's Republic of China
Email guibsdoctor@sina.com

Jian-Ming Ouyang
Institute of Biomineralization and Lithiasis Research, Jinan University, Guangzhou 510632, People's Republic of China
Email toyjm@jnu.edu.cn

nucleation, growth, and aggregation of CaOx crystals are inhibited and the formation and recurrence of CaOx stones are reduced. The recurrence rate among patients taking K_3cit is only 20% compared with those not taking K_3cit.[8]

However, reports on the property changes of urinary crystallites from patients with CaOx stones before and after K_3cit intake are very limited. The relationship between these changes and the formation of stones is also unknown. Therefore, the property changes of urinary nanocrystallites were studied in 13 patients with history of CaOx stones ("CaOx stone formers") before and after K_3cit intake, to clarify the relationship between urinary crystallites and urolithiasis, and promote clinical suppression.

Materials and methods

Reagents and instruments

The absolute ethanol, sodium azide (NaN_3), and formaldehyde (36%, v/v) used were of analytical purity. All glass vessels were cleaned with double-distilled water.

X-ray diffraction (XRD) results were recorded on a D/max-γA 2400 X-ray diffractometer (Rigaku, Tokyo, Japan). Samples were observed with a TECNAI-10 transmission electron microscope (TEM) (Royal Philips Electronics, Amsterdam, Netherlands), at an accelerating voltage of 100 kV. Image Pro Plus 5.02 software (Media Cybernetics, Rockville, MD, USA) was used to analyze the diameter and count the number of particles in the TEM images. A Nicolet 6700 Fourier-transform infrared (FT-IR) spectrometer (Thermo Fisher Scientific, Waltham, MA, USA), and a Zetasizer Nano ZS nanoparticle size and Zeta potential analyzer (Malvern Instruments Ltd, Malvern, UK) were also used.

Collection and treatment of urine

The participants in the study were 13 lithogenic patients (nine men and four women; mean age = 54.1 years, range = 24–71 years) and 13 randomly selected healthy humans with no prior history of urinary stones (nine men and four women; mean age = 38.6 years, range = 23–56 years).

Fresh urine from the CaOx-stone-forming patients was collected before and a week after K_3cit intake (dosage = 2.538 g/d). The citrate treatment lasted for 2 weeks, starting 2 days before surgery, and the urine was collected after 7 days of treatment. After detecting the pH, 2% (w/v) NaN_3 solution (10 mL/L urine sample) was added to the urine samples as antiseptic. Anhydrous alcohol (V_{urine}:$V_{anhydrous\ alcohol}$ = 3:2) was then added to 30 mL of each urine sample, stirred, and left to stand for 30 minutes. The purpose of the addition of alcohol was to remove the proteins in the urine. Alcohol can denaturalize and deposit the proteins, which can interfere with the observation of urinary crystallites by TEM as well as with the identification of peaks by XRD and FT-IR. The urine was then filtered through a 1.2 μm microporous membrane.

Collection and component characterization of urinary calculus

Urinary stones were collected after surgery, cleared with double-distilled water, and placed in a dust-free incubator at 50°C for drying. The urinary stones were then ground into powder with an agate mortar for XRD and FT-IR characterization. Results showed that the urinary stones were mainly composed of CaOx with a mass fraction of 90% to 100%. The other components of the urinary stones included β-calcium phosphate and uric acid.

Measurement of zeta potential (ζ) and particle size

The above-filtered urine samples were ultrasonicated for 3 minutes to destroy any possible crystal agglomerations. Subsequently, to detect the ζ and particle sizes of the urinary crystallites, about 1.5 mL from each sample of treated urine was immediately injected into the cell of a ζ analyzer, and another 1.5 mL was injected into the cell of a nanoparticle size analyzer.

Characterization of urine crystallite components

XRD and FT-IR detection of urinary crystallites

About 100 μL of spare urine from each sample was placed on clean glass slides using a microsyringe. The glass slides were then dried in an oven at 50°C ± 5°C for 2 hours to volatilize the urine. This process was repeated three times. Nanocrystallites were then deposited onto the glass slides. Subsequently, the glass slides were slowly immersed in distilled water at a 45° angle and gently shaken for 1 minute to remove the soluble fractions of sodium chloride and urea. After carefully removing the glass slides, water from the edge of the slides was dried using an absorbent paper, and the slides were again dried at 50°C ± 5°C in a vacuum desiccator for 1 day, for further XRD and FT-IR characterization.

TEM detection of urinary crystallites

About 5 μL of the above spare urine from each sample was placed in a copper mesh. The copper mesh was stored in a desiccator for 24 hours and then examined by TEM.

Determination of citric acid, gycosaminoglycans (GAGs), and uric acid (UA) in the urine

The Alcian blue colorimetric method and ammonium metavanadate-assisted catalytic-kinetic spectrophotometry were used to detect the contents of GAGs and citrate in urine.[9,10] Using a spectrophotometer, the UA content was determined by its ability to reduce Fe (III) to Fe (II), which can then coordinate with phenanthroline to produce orange-red complexes.[11]

Statistical analysis

The experimental data were analyzed using SPSS version 16.0 software (IBM, Armonk, NY, USA). The experimental data were expressed as the mean ± standard deviation. Data differences between two groups were analyzed by a *t*-test, and the *P* value was used to assess the statistical significance. $P < 0.05$ was deemed to indicate a significant difference, $P < 0.01$ indicated an extremely significant difference, and $P > 0.05$ indicated no significant difference.

Results and discussion

Powder XRD analysis of urinary crystallites before and after K_3cit intake

The urinary crystallites of all 13 cases of CaOx stone formers before and after K_3cit intake were analyzed using XRD. Three representative results are shown in Figure 1. The results show the following:

1. Before K_3cit intake, the main components of the urinary crystallites of the CaOx stone formers included UA, β-calcium phosphate, and calcium oxalate monohydrate (COM) (Figure 1A, C, and E).

   The diffraction peaks located at 3.86, 3.53, and 2.73 Å were assigned to the $(\bar{2}11)$, (301), and (202) plane of UA, respectively.[12] The peaks at 2.84, 2.49, and 1.98 Å were assigned to the (121), (112), and $(\bar{3}03)$ plane of COM, respectively. The diffraction peaks at 5.23, 3.00, and 2.65 Å were assigned to the (110), (300), and (1112) plane of β-calcium phosphate, respectively (Figures 1A and E).
2. After 1 week of K_3cit intake, the number of diffraction peaks of urinary crystallites decreased (Figure 1B, D, and F). This result showed that the species of urinary crystallites decreased after taking K_3cit.[13]
3. The intensity of the diffraction peaks of urinary crystallites weakened after K_3cit intake. This result showed that the mass of crystallites significantly declined after K_3cit intake.[13]

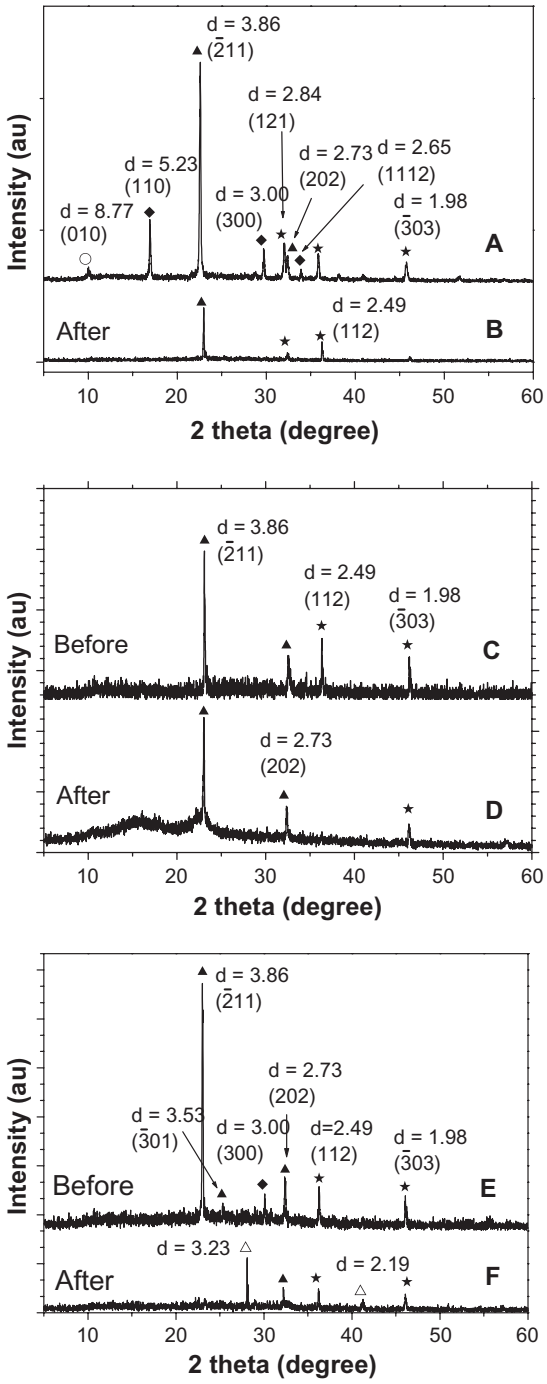

Figure 1 XRD patterns of urinary nanocrystallites of the three CaOx stone-forming patients before (**A**, **C** and **E**) and after (**B**, **D** and **F**) K_3cit intake.
Notes: ✱: calcium oxalate monohydrate; ▲: uric acid; △: monosodium urate; ♦: β-$Ca_3(PO_4)_2$; ○: $MgNH_4PO_4{\cdot}6H_2O$.
Abbreviations: XRD, X-ray diffraction; CaOx, calcium oxalate; K_3cit, potassium citrate.

Compared with the XRD patterns of urinary crystallites before K_3cit intake, the diffraction peak of UA at d = 3.86 and 2.73 Å abated (Figure 1B and D) or disappeared (Figure 1F) after K_3cit intake. This result indicated that the amount of UA in urine significantly decreased.

The citrate excreted in urine after K_3cit intake can alkalize urine, which can increase the urine pH and transform the majority of UA to urate, whose larger solubility significantly reduces the mass of UA.

Similarly, the diffraction peaks of COM at 2.49 and 1.98 Å also decreased (Figure 1B) or disappeared (Figure 1D and F), suggesting that the content of COM crystallites also decreased after K_3cit intake. K_3cit is a strong complex agent that can combine with Ca^{2+} ions to form soluble calcium citrate, which reduces the saturation degree of CaOx in urine thus inhibiting the formation of CaOx crystals. Consequently, the amount of CaOx crystallites in the urine decreased after K_3cit intake for 1 week.

4. After K_3cit intake, new diffraction peaks of monosodium urate appeared. As shown in Figure 1F, the diffraction peaks assigned to UA and COM abated or disappeared after K_3cit intake. However, new diffraction peaks appeared at 3.23 and 2.19 Å because of the appearance of monosodium urate.[14] These results indicated that monosodium urates were present in the urine.

Representative FT-IR spectra of urinary crystallites before and after K_3cit intake

The changes in urinary crystallites components were examined by FT-IR spectroscopy. The representative spectra are shown in Figure 2.

1. Before K_3cit intake, the peaks detected at 1668, 1454, and 524 cm^{-1} indicated the presence of UA.[15,16] The peaks of coordinated water were located at 3488 cm^{-1} to 3219 cm^{-1}. These broad peaks were attributed to the symmetrical stretching vibration and asymmetrical stretching vibration of OH^- of coordinated water molecules. The peaks at 1332, 781, and 592 cm^{-1} were characteristic adsorptions of COM (Figures 2C and E).

   The absorption peaks of β-calcium phosphate were also detected in some samples. As shown in Figure 2A, 1160 cm^{-1} was attributed to the O—P—O symmetric stretching vibration and 1080 cm^{-1} was attributed to the PO_4^{3-} asymmetric vibration absorption peak. As shown in Figure 2C, 989 cm^{-1} was attributed to the PO_4^{3-} symmetric vibration absorption peak.[17]

   Before K_3cit intake, the main components of urinary crystallites were UA, COM, and β-calcium phosphate, which were consistent with the XRD results.
2. The absorption peaks after K_3cit intake changed as follows (Figure 2B, D, and F):
   a. The absorption peak intensity weakened or even disappeared. The number of absorption peaks was significantly lower after K_3cit intake (Figure 2B) than before K_3cit intake (Figure 2A). The absorption peaks of the in-plane bending vibration of O=C$^-$O$^-$ (γ_{as}(COO$^-$)) at 935 and 885 cm^{-1} for COM disappeared, and the stretching vibration of C-N for UA at 1403 cm^{-1} weakened.

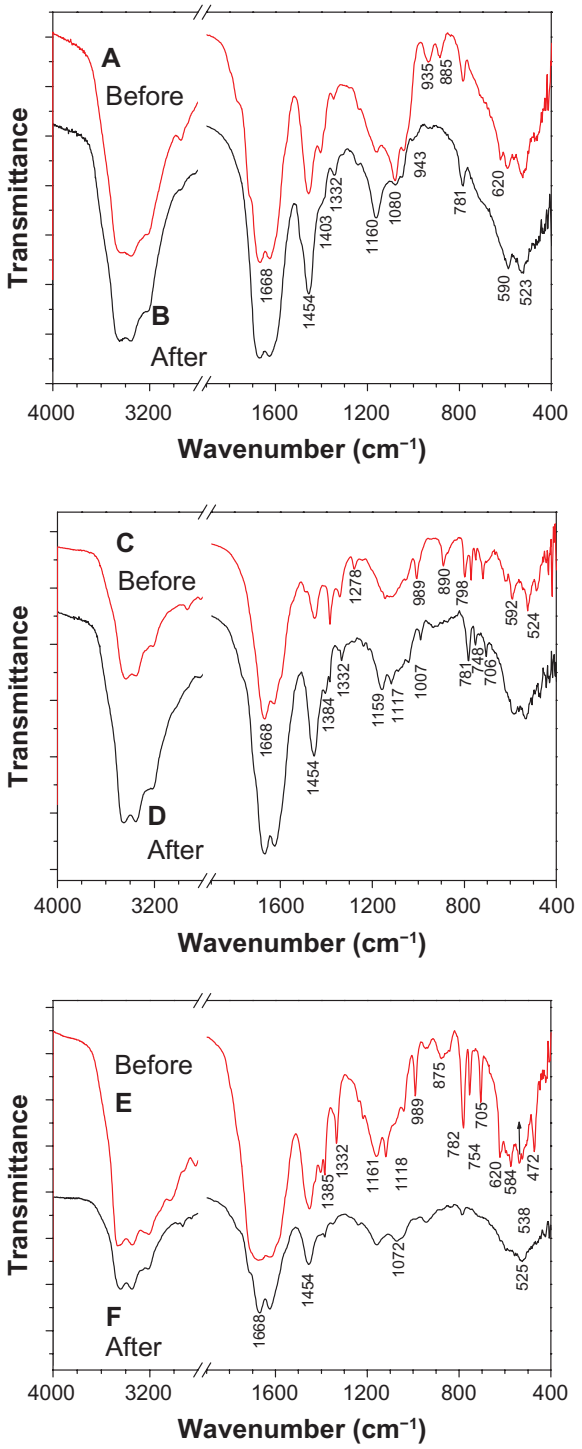

Figure 2 FT-IR spectra of urinary nanocrystallites of the three CaOx stone-forming patients before (**A**, **C**, and **E**) and after (**B**, **D**, and **F**) K_3cit intake.
Abbreviations: FT-IR, Fourier-transform infrared (spectrometer); CaOx, calcium oxalate; K_3cit, potassium citrate.

When comparing Figure 2C and D or Figure 2E and F, the stretching vibration of C=O of COM at 1384 and 1332 cm^{-1}, the stretching vibration of C–C of COM at 782 cm^{-1}, the stretching vibration of C=O of UA at 1118 cm^{-1}, and the peaks of UA at 875, 705, 620, 538, and 472 cm^{-1} in the fingerprint region, all either weakened or disappeared.

b. After K_3cit intake, the absorption peaks of monosodium urate and β-calcium phosphate either appeared or increased in intensity. Before K_3cit intake (Figure 2C), only the symmetric stretching vibration peak of O–P–O at 1159 cm^{-1} and PO_4^{3-} at 989 cm^{-1} were present. However, after K_3cit intake (Figure 2D), new absorption peaks appeared at 1007 cm^{-1} for phosphate, as well as at 2927 and 798 cm^{-1} for urate.[18]

Therefore, the FT-IR results were consistent with those of the XRD.

Property changes of urine before and after K_3cit intake

Changes in citrate, GAGs, and UA excretion

After K_3cit intake for 1 week, the citrate excretion from the urine of all 13 cases of CaOx stone formers increased from 264 ± 74 mg/L to 381 ± 109 mg/L (Figure 3E), and UA excretion decreased from 563 ± 91 mg/L to 393 ± 86 mg/L (Figure 3F). No significant difference was observed before and after K_3cit intake ($P > 0.05$). However, the excretion of GAGs from urine increased from 5.18 ± 0.82 mg/L to 11.81 ± 1.62 mg/L. These differences in GAGs excretion before and after K_3cit intake were significant ($P < 0.05$).

Changes in urine pH before and after K_3cit intake

Before K_3cit intake, the urine pH was between 5.2 and 6.7 (Figure 3A), with an average value of 5.96 ± 0.43 (Table 1). At 1 week post-K_3cit intake, the urine pH increased to an average value of 6.46 ± 0.50; however, this difference was not significant ($P > 0.05$). After K_3cit intake, the urine pH (6.46 ± 0.50) was close to that of the healthy controls (6.28 ± 0.30) ($P > 0.05$).

The increase in urine pH was caused by the increase of K_3cit excretion after K_3cit intake. K_3cit is an alkaline salt and can alkalize urine.

Size changes of urinary crystallites before and after K_3cit intake

The particle size distribution and average diameter of urinary nanocrystallites from the 13 CaOx stone-forming patients before and after K_3cit intake were studied using a nanoparticle size analyzer. Before K_3cit intake, the average particle size of urinary nanocrystallites in the 13 cases was 524 ± 320 nm (Figure 3B). After K_3cit intake for 1 week, the particle size decreased to 354 ± 173 nm. Figure 4 showed the particle size distribution of urinary crystallites of two CaOx stone patients before and after K_3cit intake. Before K_3cit intake, the peak particle size values were 688 and 106 nm, with an average size of 293 nm (Figure 4A), as well as 7.5, 80, and 955 nm, with an average size of 432 nm (Figure 4C), respectively. After K_3cit intake, the peak particle size values were accordingly reduced to 19, 98, and 394 nm, with an average size of 146 nm (Figure 4B), as well as 29, 123, and 495 nm, with an average size of 220 nm (Fig. 4D), respectively.

Citrate excretions in the urine increased from 264 ± 74 mg/L before K_3cit intake to 381 ± 109 mg/L at 1 week after commencing K_3cit intake (Figure 3E). On one hand, as an inhibitor of CaOx crystallization, citrate can close the growth sites of CaOx crystals, thereby inhibiting the growth and aggregation of CaOx crystals and ultimately decreasing the size of urinary crystallites. On the other hand, K_3cit chelated Ca^{2+} ions and dissolved the CaOx crystallites.

ζ change of urinary crystallites before and after K_3cit intake

Figure 3C shows the ζ change of urinary crystallites from CaOx stone-forming patients before and after K_3cit intake. The average ζ value of urinary crystallites in the 13 CaOx stone formers were –4.85 ± 2.87 mV before K_3cit intake and –8.77 ± 3.03 mV after K_3cit intake; the latter was close to the ζ value –8.89 ± 2.23 mV of healthy subjects ($P > 0.05$). The ζ value became negative after K_3cit intake because of the following:

1. As shown in Figure 3E, the citrate excretion in urine was increased after K_3cit intake. As an anion inhibitor, citrate can be adsorbed on the positively charged surface of crystallites, such as COM, which can increase the negative charges on the crystallite surface. Thus, the ζ becomes negative.
2. After K_3cit intake, the excretion and activity of Tamm-Horsfall protein (TH protein) increased.[19] TH protein is also an anionic protein that enables the ζ of CaOx crystals to turn negative.
3. After K_3cit intake, the urine pH increased, which subsequently increased the ionization of acidic substances and the amount of negatively charged anionic species in urine. For example, the increase in pH can promote the ionization of citric acid in urine, causing the concentration of trivalent anionic citrate (cit^{3-}) to increase. The pH increase can also convert uric acid into urate and cystine into its salt, thereby further increasing the number of negatively charged species.

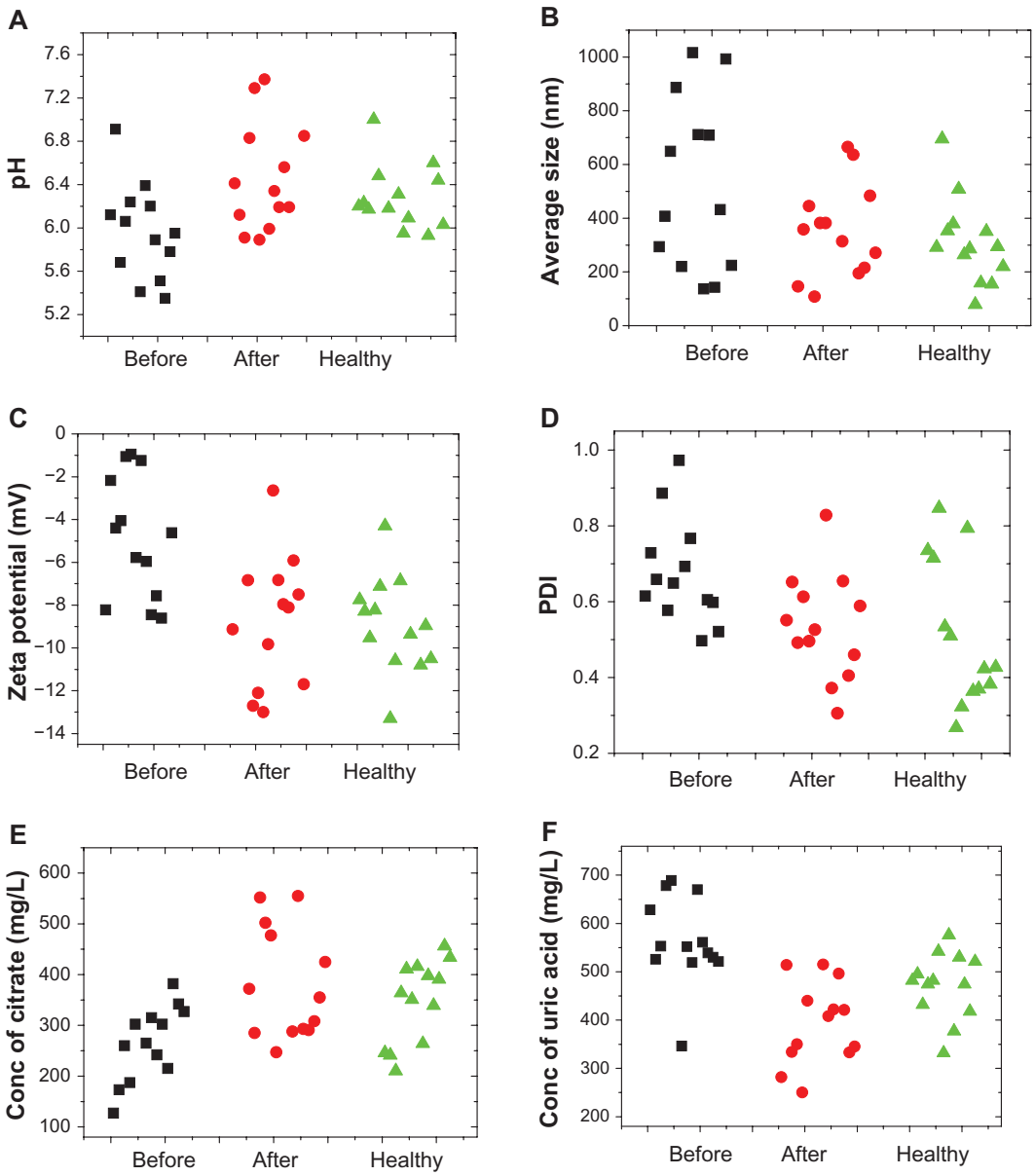

Figure 3 Comparison between the properties of urine and urinary crystallites from healthy controls and patients with CaOx stones before and after K_3cit intake: urinary pH (**A**); average particle size (**B**); ζ (**C**); PDI (**D**); amount of excreted citrate (**E**); and amount of excreted UA (**F**).
Note: n = 13.
Abbreviations: CaOx, calcium oxalate; K_3cit, potassium citrate; ζ, zeta potential; PDI, polydispersity index; UA, uric acid.

4. With increased pH, the OH^- ions in the urine increased. On the other hand, the crystallite surfaces were negatively charged because of the adsorbance of anionic inhibitors under a basic condition. Consequently, the thickness of the electric double-layer between the OH^- ions and urinary crystallites increased. According to the DLVO colloid flocculation theory, the repulsive energy of the electric double layer depends on the thickness of the electric double layer. An increase in thickness of the electric double layer increases the repulsive energy, thereby leading to an increased absolute value of the ζ.[20,21]

After the ζ of the urinary crystallite surfaces became negative, the electrostatic repulsion increased, thereby inhibiting the growth and aggregation of urinary crystallites. These anions also closed the growth sites of crystals to further inhibit crystal growth.

Stability difference between urinary crystallites before and after K_3cit intake

Intensity-autocorrelation curve changes

The nanocrystallites particles in urine are in continuous Brownian movement. Brownian movement is a random fluc-

Table 1 Comparison of the properties of urine and urinary crystallites from healthy controls and CaOx stone-forming patients before and after K_3cit intake (n = 13)

	Before K_3cit	After K_3cit	Control	P[a]
K_3cit excretion, mg/L	264 ± 74	381 ± 109	348 ± 82	$P > 0.05$
GAG excretion, mg/L	5.18 ± 0.82	11.81 ± 1.62	9.80 ± 1.83	$P < 0.05$*
UA excretion, mg/L	563 ± 91	393 ± 86	472 ± 68	$P > 0.05$
Urine pH	5.96 ± 0.43	6.46 ± 0.50	6.28 ± 0.30	$P > 0.05$
particle size, nm	524 ± 320	354 ± 173	310 ± 160	$P < 0.05$*
ξ, mV	–4.85 ± 2.87	–8.77 ± 3.03	–8.89 ± 2.23	$P > 0.05$
PDI	0.67 ± 0.14	0.53 ± 0.19	0.51 ± 0.14	$P > 0.05$
Decay time T, ms	11.4 ± 3.2	4.3 ± 1.7	2.8 ± 0.7	$P < 0.05$*

Notes: Values are shown as mean ± standard deviation.
[a]Comparisons were made against CaOx stone patients before and after K_3cit intake. *Statistically significant comparisons.
Abbreviations: CaOx, calcium oxalate; K_3cit, potassium citrate; GAG, gycosaminoglycans; UA, uric acid; ξ, zeta potential; PDI, polydispersity index.

tuation motion that denotes the rate of light intensity change in relation to particle size. A smaller particle corresponds to a faster Brownian movement, leading to a faster scattering intensity change and an inferior signal correlation as well as quick variations in the attenuation of curves.[22–24] A faster attenuation of the autocorrelation curve corresponds to a steeper curve and shorter decay time. By contrast, larger particles correspond to slower Brownian movement, leading to a slower scattering intensity change and corresponding in turn, to better signal correlations and slower attenuation of the autocorrelation curve.

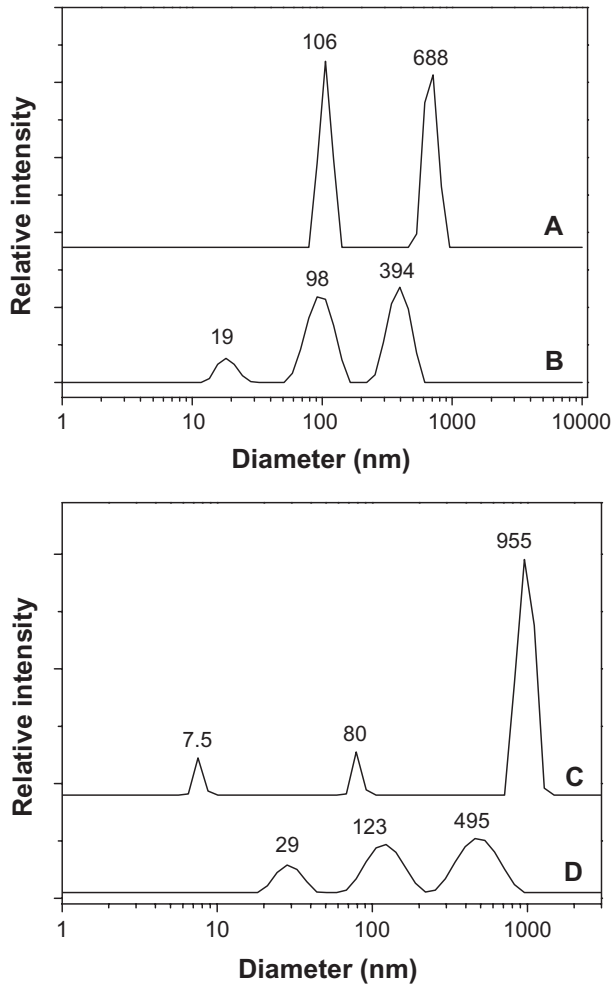

Figure 4 Particle size distribution of urinary crystallites of two CaOx stone patients before (**A** and **C**) and after (**B** and **D**) K_3cit intake.
Abbreviations: CaOx, calcium oxalate; K_3cit, potassium citrate.

Before K_3cit intake, the baseline of the intensity-autocorrelation curves was coarser (Figure 5A) and the attenuation of the curves was slower. This result indicated that urine particles were larger before K_3cit intake or that aggregated crystallites existed, which conformed to the detection result of the particle size.

After K_3cit intake, the baseline of the intensity-autocorrelation curves of the urine nanocrystallites was smoother, and the attenuation of the curves was faster (Figure 5B). The attenuation time was also reduced to 4.3 ± 1.7 ms (Table 1). This result suggested that the particles of crystallites in urine were smaller.

Polydispersity index (PDI) changes

PDI is a parameter that characterizes the width of the particle size distribution. A smaller PDI value corresponds to a narrower particle size distribution range and more uniform particles for the tested sample. For standard samples or truly monodispersed samples, PDI < 0.05, whereas PDI = 0.05–0.08 if the samples are almost monodispersed. When the PDI = 0.08–0.7, the samples are in moderate dispersion. The PDI of the sample values within this range is suitable for detection of particle size and particle size distribution, using a nanoparticle size analyzer. If the PDI > 0.7 of the sample, the distribution range is too wide for a nanoparticle size analyzer, based on the principle of dynamic light scattering.

Before K_3cit intake, the PDI of the urinary crystallites of all stone formers was greater than 0.5 (Figure 3D), with an average value of 0.67 ± 0.14. This result indicated that the

size of these crystallites was uneven, that the urine system was unstable, and that the crystallites easily aggregated. However, the PDI decreased to 0.53 ± 0.19 after K_3cit intake, indicating that the distribution range of the urinary crystallites became narrower and that the particle size was homogenized.

Decay time changes

As shown in Table 1, the order of decay time of the different kinds of urinary crystallites was as follows: the decay time in patients before K_3cit intake (11.4 ± 3.2 ms) > the decay time in patients after K_3cit intake (4.3 ± 1.7 ms) > the decay time in healthy controls (2.8 ± 0.7 ms).

This result suggested that the average particle size of the urinary crystallites before K_3cit intake was larger than that after K_3cit intake.[25,26] These results were attributed to the lower concentration and activity of inhibitors in the urine of stone-forming patients, preventing the adsorption of most crystallites by inhibitor molecules. A stronger electrostatic interaction also exists between these free crystallites; thus, these crystallites aggregated more easily than those of the controls. Compared with the urine before K_3cit intake, the aggregation degree of crystallites was reduced after K_3cit intake, thus reducing the risk of stone formation.

After the absolute ζ value on the crystallite surfaces increased, the electrostatic repulsive forces also increased, and the particles were not easy to aggregate. Therefore, K_3cit increased the stability of the urine system and reduced calculus formation.

Changes in appearance of urinary crystallites before and after K_3cit intake

As shown in Figure 6, the TEM detection results further confirmed the above results. Urinary crystallites from CaOx stone formers before K_3cit intake exhibited sharp edges and corners, large size differences ranging from a few nanometers to 1000 nm, and significant aggregation of crystallites (Figure 6A and B). After K_3cit intake, the crystallites became blunt, decreased in size, and showed less aggregation (Figure 6C and D). The changes in appearance and size of the urinary crystallites before and after K_3cit intake were due to the following four reasons:

1. First, the K_3cit concentration increased in the urine after K_3cit intake. K_3cit is a chelating agent. It can combine with Ca^{2+} ions in urine to form soluble calcium citrate and reduce the Ca^{2+} ion concentration and CaOx saturation in urine. After the CaOx saturation decreased, the deposited CaOx crystallites decreased, and the growth and aggregation of CaOx crystallites were also inhibited. Thus, the size of urinary crystallites was reduced.
2. The increase in urine pH not only transformed UA into urate, whose solubility is much larger than that of UA, but also decreased UA deposition. The increase in urine pH also decreased the heterogeneous nucleation of CaOx crystals, as these are often caused by UA crystals.[27]
3. A strong precipitation–dissolution equilibrium existed between K_3cit and CaOx crystallites. The Ca^{2+} ions on

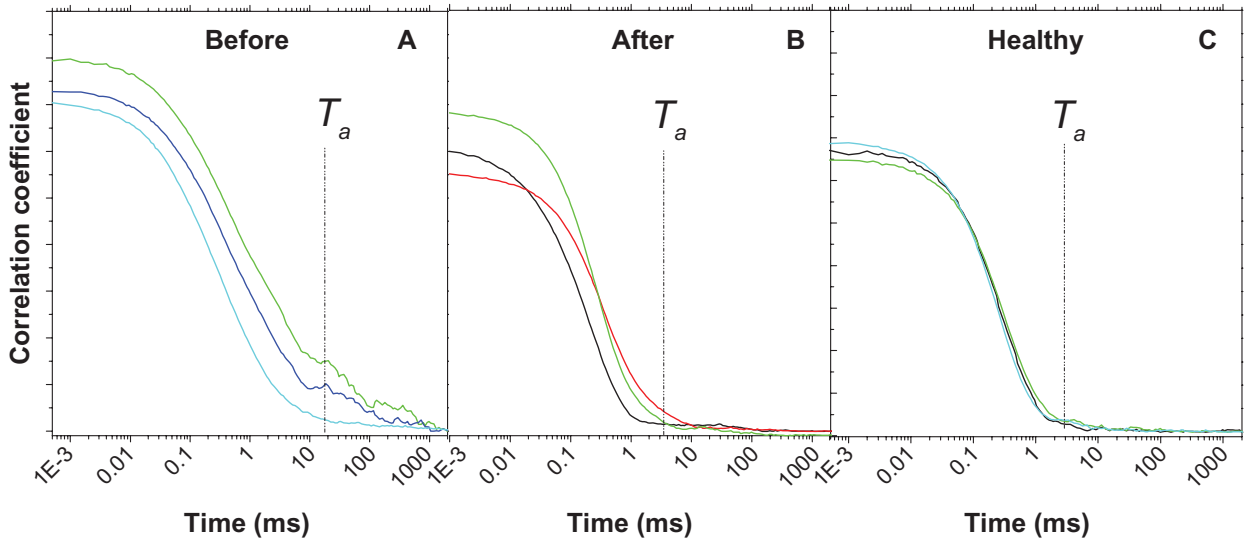

Figure 5 Attenuation curve of the intensity autocorrelation function of urinary crystallites from three patients with CaOx stones before (**A**) and after (**B**) K_3cit intake, and three healthy controls (**C**).
Abbreviations: CaOx, calcium oxalate; K_3cit, potassium citrate; T_a, decay time.

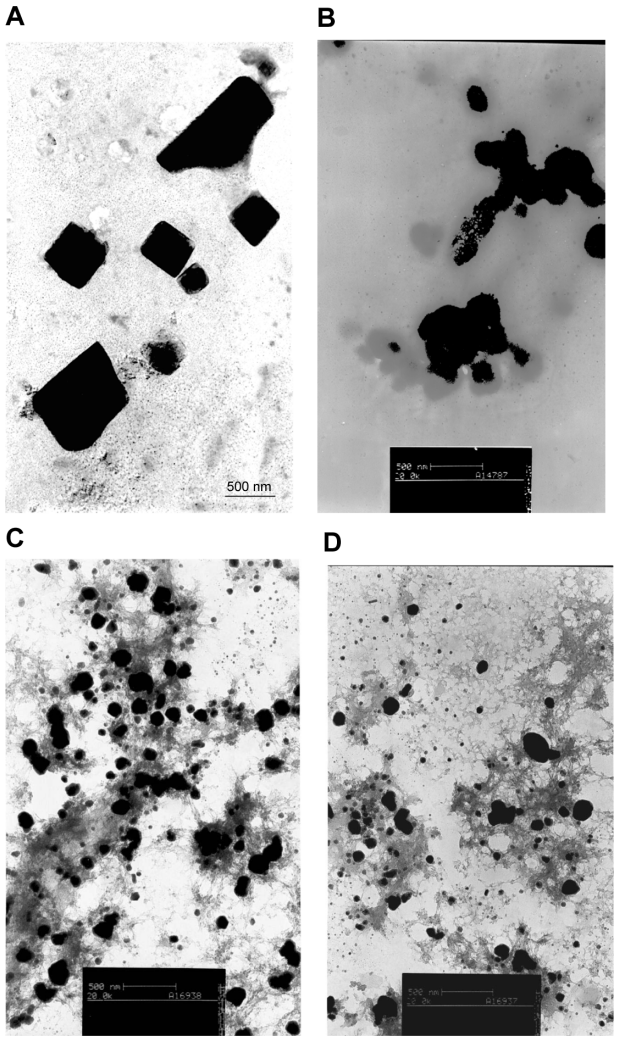

Figure 6 TEM images of urinary nanocrystallites of two CaOx stone-forming patients before (**A** and **B**) and after (**C** and **D**) K_3cit intake.
Note: Bar: 500 nm.
Abbreviations: TEM, transmission electron microscope; CaOx, calcium oxalate; K_3cit, potassium citrate.

the surface of CaOx crystallites, particularly the Ca^{2+} ions on the peripheries and edges, were constantly dissolved by K_3cit. The dissolved Ca^{2+} ions also constantly precipitated to the surface of crystallites. This continuous precipitation-dissolution process made the crystallites blunt (Figure 6C and D).

4. The increase in pH can strengthen the inhibitory activity of some components in urine, such as TH protein and pyrophosphate.[28,29] TH protein plays dual roles in CaOx crystallite aggregation. TH protein promotes crystallite aggregation at lower pH but inhibits aggregation at higher pH.[19] Accordingly, in this study, the aggregation of urinary crystallites decreased after K_3cit intake. Therefore, the increase in urinary pH was conducive to the prevention of CaOx stone formation.

Conclusion

The main components of the urinary crystallites of CaOx stone-forming patients were UA, COM, and β-calcium phosphate. Before K_3cit intake, the edges and corners of the crystallites were sharp, their sizes ranged from a few nanometers to 1000 nm, and they showed significant aggregation. By contrast, at 1 week post-K_3cit intake, the urine pH increased, the species and mass of urinary crystallites significantly decreased, the crystallite morphology became blunt, the absolute value of ζ on the crystallite surface increased, the average size of crystallites decreased, and the aggregation of crystallites significantly decreased. All these changes helped inhibit the urinary crystallite deposition and CaOx stone formation.

Acknowledgments

This research was supported by the Natural Science Foundation of China (81170649).

Disclosure

The authors report no conflicts of interest in this work.

References

1. Grohe B, Hug S, Langdon A, et al. Mimicking the biomolecular control of calcium oxalate monohydrate crystal growth: effect of contiguous glutamic acids. *Langmuir*. 2012;28(33):12182–12190.
2. Yao XQ, Ouyang JM, Peng H, Zhu WY, Chen HQ. Inhibition on calcium oxalate crystallization and repair on injured renal epithelial cells of degraded soybean polysaccharide. *Carbohydr Polymers*. 2012;90(1):392–398.
3. Peng H, Ouyang JM, Yao XQ, Yang RE. Interaction between submicron COD crystals and renal epithelial cell. *Int J Nanomed*. 2012;7:4727–4737.
4. Daudon M, Hennequin C, Boujelben G, Lacour B, Jungers P. Serial crystalluria determination and the risk of recurrence in calcium stone formers. *Kidney Int*. 2005;67(5):1934–1943.
5. He JY, Deng SP, Ouyang JM. Morphology, particle size distribution, aggregation, and crystal phase of nanocrystallites in urine of healthy persons and lithogenic patients. *IEEE Trans Nanobioscience*. 2010;9(2):156–163.
6. Gui BS, Huang ZJ, Xu XJ, Li MR, He JY, Ouyang JM. Measurement of urine crystallites and its influencing factors by nanoparticle size analyzer. *J Nanosci Nanotechnol*. 2010;10(8):5232–5241.
7. Mechlin C, KalorinC, Asplin J, White M, Splenda®. Improves tolerance of oral potassium citrate supplementation for prevention of stone formation: results of a randomized double-blind trial. *J Endourol*. 2011;25(9):1541–1545.
8. Fuselier HA, Moore K, Lindberg J, et al. Agglomeration inhibition reflected stone-forming activity during long-term potassium citrate therapy in calcium stone formers. *Urology*. 1998;52(6):988–994.
9. Whiteman P. The quantitative determination of glycosaminoglycans in urine with Alcian Blue 8GX. *Biochem J*. 1973;131(2):351–357.
10. Ding S-F, Jin H-M, Zhu SP. Catalytic activation dynamic determination of citric acid. *Chin J Health Lab Tech*. 2009;19(7):1520–1521.
11. Zuo Y, Wang C, Zhou J, Sachdeva A, Ruelos VC. Simultaneous determination of creatinine and uric acid in human urine by high-performance liquid chromatography. *Anal Sci*. 2008;24(12):1589–1592.

12. King M, McClure WF, Andrews LC. *Powder Diffraction File Alphabetic Index, Inorganic Phases/Organic Phases*. Newtown Square: International Center for Diffraction Data; 1992.
13. Jin Y, Sun XS, Xue J. *X-ray Diffraction Analysis Techniques*. Beijing: National Defence Industrial Press; 2008.
14. Cytron S, Kravchick S, Sela BA, et al. Fiberoptic infrared spectroscopy: a novel tool for the analysis of urine and urinary salts in situ and in real time. *Urology*. 2003;61(1):231–235.
15. Benramdane L, Bouatia M, Idrissi MOB, Draoui M. Infrared analysis of urinary stones, using a single reflection accessory and a KBr pellet transmission. *Spectrosc Lett*. 2008;41(2):72–80.
16. Jing Z, GuoZeng W, Ning J, JiaWei Y, Yan G, Fang Y. Analysis of urinary calculi composition by infrared spectroscopy: a prospective study of 625 patients in eastern China. *Urol Res*. 2010;38(2):111–115.
17. Frost RL, Xi Y, Scholz R, Belotti FM, Alberto Dias Menezes Filho L. Raman and infrared spectroscopic characterization of beryllonite, a sodium and beryllium phosphate mineral-implications for mineral collectors. *Spectrochim Acta Biomol Spectrosc*. 2012;97:1058–1062.
18. Verdesca S, Fogazzi GB, Garigali G, Messa P, Daudon M. Crystalluria: prevalence, different types of crystals and the role of infrared spectroscopy. *Clin Chem Lab Med*. 2011;49(3):515–520.
19. Hess B, Zipperle L, Jaeger P. Citrate and calcium effects on Tamm-Horsfall glycoprotein as a modifier of calcium oxalate crystal aggregation. *Am J Physiol*. 1993;265(6 Pt 2):F784–F791.
20. Song X, Jiang N, Li Y, Xu D, Qiu G. Synthesis of CeO_2-coated SiO_2 nanoparticle and dispersion stability of its suspension. *Mater Chem Phys*. 2008;110:128–135.
21. Deng XC, Luo JS, Tang YJ, Han SJ, Li K, Zhang HL. Dispersion and classification of nano-cu powder. *Metallic Functional Materials*. 2010;(3):37–41.
22. Frisken B. Revisiting the method of cumulants for the analysis of dynamic light-scattering data. *Appl Opt*. 2001;40(24):4087–4091.
23. Gui BS, Huang ZJ, Xu XJ, Li MR, He JY, Ouyang JM. Measurement of urine crystallites and its influencing factors by nanoparticle size analyzer. *J Nanosci Nanotechnol*. 2010;10(8):5232–5241.
24. Lin HM, Shao YH, Qu JL, Yin J, Chen SP, Niu HB. Study on wide-field fluorescence sectioning microscopy based on dynamic speckle illumination. *Acta Phys Sin*. 2008;57(12):7641–7649.
25. Kinjo M, Sakata H, Mikuni S. Fluorescence correlation spectroscopy example: shift of autocorrelation curve. *Cold Spring Harb Protoc*. 2011; 10:1267–1269.
26. Murphy DL, Beretvas SN, Pituch KA. The effects of autocorrelation on the curve-of-factors growth model. *Struct Equ Modeling*. 2011;18(3): 430–448.
27. Allie S, Rodgers A. Effects of calcium carbonate, magnesium oxide and sodium citrate bicarbonate health supplements on the urinary risk factors for kidney stone formation. *Clin Chem Lab Med*. 2003;41(1):39–45.
28. Pak CY. Citrate and renal calculi: an update. *Miner Electrolyte Metab*. 1994;20(6):371–377.
29. Caudarella R, Vescini F. Urinary citrate and renal stone disease: the preventive role of alkali citrate treatment. *Arch Ital Urol Androl*. 2009; 81(3):182–187.